

Fluorinated Pickering Emulsions Impede Interfacial Transport and Form Rigid Interface for the Growth of Anchorage-Dependent Cells

Ming Pan,[†] Liat Rosenfeld,[‡] Minkyu Kim,[‡] Manqi Xu,^{‡,§} Edith Lin,^{||} Ratmir Derda,^{||} and Sindy K. Y. Tang^{*,‡}

[†]Department of Material Science and Engineering, Stanford University, Stanford, California 94305-2004, United States

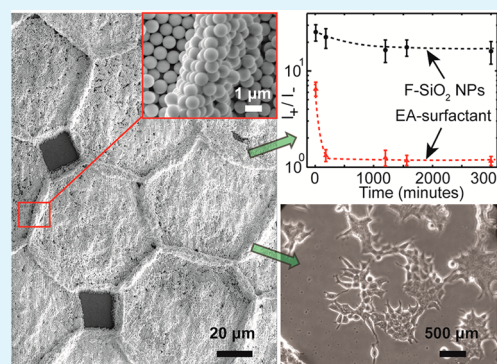
[‡]Department of Mechanical Engineering, Stanford University, Stanford, California 94305-2004, United States

[§]Undergraduate Visiting Research Program, School of Engineering, Stanford University, Stanford, California 94305-2004, United States

^{||}Department of Chemistry, University of Alberta, Edmonton, Alberta T6G 2R3, Canada

S Supporting Information

ABSTRACT: This study describes the design and synthesis of amphiphilic silica nanoparticles for the stabilization of aqueous drops in fluorinated oils for applications in droplet microfluidics. The success of droplet microfluidics has thus far relied on one type of surfactant for the stabilization of drops. However, surfactants are known to have two key limitations: (1) interdrop molecular transport leads to cross-contamination of droplet contents, and (2) the incompatibility with the growth of adherent mammalian cells as the liquid–liquid interface is too soft for cell adhesion. The use of nanoparticles as emulsifiers overcomes these two limitations. Particles are effective in mitigating undesirable interdrop molecular transport as they are irreversibly adsorbed to the liquid–liquid interface. They do not form micelles as surfactants do, and thus, a major pathway for interdrop transport is eliminated. In addition, particles at the droplet interface provide a rigid solid-like interface to which cells could adhere and spread, and are thus compatible with the proliferation of adherent mammalian cells such as fibroblasts and breast cancer cells. The particles described in this work can enable new applications for high-fidelity assays and for the culture of anchorage-dependent cells in droplet microfluidics, and they have the potential to become a competitive alternative to current surfactant systems for the stabilization of drops critical for the success of the technology.



KEYWORDS: Pickering emulsion, droplet microfluidics, nanoparticles, amphiphilicity, biocompatibility

1. INTRODUCTION

Droplet microfluidics, in which droplets act as individual reactors, has enabled drastic improvements in the throughput of biochemical processes including digital polymerase chain reaction (PCR),¹ directed evolution of enzymes,² and screening of antibiotics.³ The technology and all related applications have relied critically on the availability of a single type of surfactant to stabilize the drops against coalescence. However, the surfactant system is known to have two key limitations: (1) undesirable interdrop molecular transport, which causes cross contamination of droplet contents and severely compromises the accuracy of droplet assays and (2) incompatibility with the growth of adherent cells. Here, we describe the use of amphiphilic silica nanoparticles, instead of surfactants, for stabilizing aqueous drops in fluorinated oils. We show that these nanoparticles are effective in overcoming the limitations of current surfactant systems.

The key assumption in droplet-based assays is that reagents remain isolated in individual droplets and cannot diffuse across the interface between a drop and the continuous phase. The

continuous phase is typically a fluorinated oil due to its gas permeability, chemical inertness, and low toxicity to cells.⁴ As the fluorinated phase is immiscible with both the aqueous and organic phases, it is generally assumed that the transport of molecules among drops is insignificant. It has been observed, however, that small and hydrophobic fluorescent molecules (e.g., resorufin) diffused and leaked out of aqueous drops through a continuous phase of fluorinated solvents (e.g., HFE-7500 or FC-40) containing nonionic fluorosurfactant made of PEG–PFPE amphiphilic block copolymer (also referred to as “EA-surfactant” from RainDance Technologies).^{5–7} The leakage process occurred over tens of seconds to a few hours.^{5–7} Such leakage has detrimental effects on the accuracy of the assay.^{6,8,9} The transport of molecules in reverse micelles formed by surfactant molecules present in the continuous phase has been confirmed to play a significant role in the leakage

Received: September 19, 2014

Accepted: October 27, 2014

Published: October 27, 2014

process.⁶ The use of surfactant concentrations below the critical micelle concentration would mitigate such leakage. Drops would become increasingly prone to coalescence, however, if low concentrations of surfactants are used. Additives such as bovine serum albumin and sugars have been added to the aqueous phase to increase the retention of molecules in drops.⁹ Hydrophilic groups (e.g., sulfonates) have also been incorporated into small molecules (e.g., coumarin) to eliminate its leakage out of the drops.⁷ Introduction of polar hydrophilic groups inevitably decreases the hydrophobicity and cell-permeability of the substrates. For cell viability substrates that hinges on cell-permeability, such change is counterproductive as it can inactivate the substrates.

Another key limitation of surfactant-based droplet systems is its incompatibility with the culture of anchorage-dependent cells.¹⁰ Culture of such cells is important in diagnostic applications that measure the susceptibility of cells to specific treatment. For example, the measurement of anticancer drug efficacy requires assays in which cells undergo several cell divisions. Anchorage-dependent cells divide only when they are attached to a rigid substrate that can resist sustained contractive forces by cells.¹¹ Interfaces laded with surfactants are not sufficiently rigid to support the growth of these cells. To provide anchorage support for cells, drops were previously pinned to a solid surface to allow cells to attach to a rigid support.^{12,13} Alternatively, surfactants that were covalently linked to gold nanoparticles modified with integrin-binding cyclic RGD peptide were synthesized.¹⁴ The synthesis of such surfactants was complex. While it was reported that ~90% of Jurkat E6.1 cells were in contact with the drop's periphery, it was unclear whether the rigidity of the water–oil interface was sufficient for cell proliferation. Cells actively sense the stiffness of the substrate and can undergo cell death if the substrate is too soft.¹¹ Despite some indication of adhesion of cells to nanoparticle-stabilized interfaces,^{14,15} to our knowledge, no report has demonstrated explicitly the proliferation of anchorage-dependent cells at water–oil interfaces.

An ideal solution to the above limitations would be to use emulsifiers that can (1) stabilize aqueous drops, (2) minimize leakage without the need to modify the content and chemistry of the aqueous phase, and (3) provide a sufficiently rigid interface for the attachment and growth of anchorage-dependent cells. In this study, we show that such criteria can be met if nanoparticles are used instead of surfactant molecules as emulsifiers. We modify the surface hydrophobicity of silica nanoparticles using silane chemistry to render the particles amphiphilic, that is, partially wetted by the aqueous phase and partially wetted by the fluororous phase. The particles are initially dispersed in a continuous phase of fluorinated oils. In the presence of an aqueous phase, the particles adsorb to the aqueous–fluororous interface. Our approach has four key advantages: (1) The synthesis of silica nanoparticles and the modification of their surface chemistry are simple compared with the synthesis of surfactants. The amphiphilic particles can be optimized to stabilize aqueous drops in multiple fluorinated oils (including HFE-7500, FC-40, and perfluoromethyldecalin (PFMD)), whereas existing block copolymer surfactants are not all soluble in perfluorinated oils. (2) As the particles are initially dispersed in the continuous phase, they do not interfere with the reagents inside the aqueous drops. The generation of monodisperse drops can be performed using standard flow-focusing nozzles.¹⁶ (3) Particles are nontoxic to bacteria and mammalian cells. (4) The rigid solid-like interface given by the

nanoparticles provides a favorable substrate for the attachment and spreading of adherent cells.

While there has been prior work on making nanoparticle-stabilized emulsions—or Pickering emulsions¹⁷—in microfluidic systems, most of these work used hydrocarbons as the continuous phase.^{15,18,19} Nanoparticles were not previously intended for the mitigation of the leakage of molecules, nor for the growth of adherent cells. We focus on silica nanoparticles instead of metallic nanoparticles here because the latter quench fluorescence from fluorophores that could be encapsulated inside the drops.²⁰ While fluorinated silica nanoparticles have been synthesized for use in superhydrophobic surfaces,^{21,22} no previous work has described the use of these nanoparticles for stabilizing liquid–liquid interfaces. Hereafter, we refer to our amphiphilic fluorinated SiO₂ nanoparticles as “F-SiO₂ NPs”.

2. MATERIALS AND METHODS

2.1. Materials. All chemicals were used as purchased without purification. Absolute ethanol (99%), tetraethyl orthosilicate (TEOS) (98%), ammonium hydroxide solution (28%), fluorescein, sodium salts of resazurin, and resorufin were purchased from Sigma-Aldrich. 1H,1H,2H,2H-perfluorooctyltriethoxysilane (FAS) (97%) was purchased from Fisher Scientific. Silica spheres of different sizes were purchased from Bangs Laboratories. K12 *Escherichia coli* and *E. coli* expressing Green Fluorescent Protein (GFP) (abbreviated as GFP *E. coli*) were obtained from the laboratory of Jianghong Rao at the Department of Radiology, School of Medicine, Stanford University.

2.2. Two-Step Synthesis of Fluorinated Silica Nanoparticles (F-SiO₂ NPs). First, 3.57 mL of TEOS was added to a solution containing 50 mL of ethanol (EtOH), 1 mL of deionized water, and 1.43 mL of NH₄OH (28 wt %). The reaction mixture was then stirred vigorously at room temperature for 12 h to yield pristine SiO₂ NPs. Then, 250 μL of FAS was added directly to every 5.25 mL of the synthesized SiO₂ NPs solution obtained above, followed by vigorous stirring at room temperature for 60 min. To terminate the reaction, 22 mL of EtOH was added to dilute the reacting solution, and the particles were washed by centrifugation at 10 000 rpm for 20 min. After three cycles of washing, the supernatant was removed and the resulting particles were desiccated overnight. The mass of the solid was weighed, and the solid was then redispersed in fluorinated solvent (HFE-7500TM (3M), FC-40 or perfluoromethyldecalin). After fluorination, the resulting particles were easily dispersible in fluorinated oil. Syringe filters (polytetrafluoroethylene (PTFE) membrane, pore size 450 nm, VWR) were used to remove the dust and aggregates present in the suspension.

2.3. Fluorination of Commercially Available Silica Particles. Silica nano- or microparticles from Bangs Lab were concentrated from the original aqueous suspension by centrifugation at 1000 rpm. After removing the supernatant, 5.36 mL of EtOH and 153.6 μL of NH₄OH were added to 10 μL of the concentrated particle suspension. Appropriate amount of FAS was added under vigorous stirring (see Supporting Information for details). After 40 min of reaction, the particles were isolated by centrifugation at 1000 rpm. Such particles were highly dispersible in fluorinated solvents and concentrations of 5% (w/w) in HFE-7500 can be obtained.

2.4. *E. coli* Cell Culture. Liquid cultures of *E. coli* were grown by picking a colony from the agar plate and dipping into a growth media which contained autoclaved LB broth with 20 μg/mL of tetracycline (for K12 *E. coli*) or 50 μg/mL of kanamycin and 0.1 mM Isopropyl β-D-1-thiogalactopyranoside (IPTG, for GFP *E. coli*). To measure the growth rate of K12 *E. coli* inside droplets stabilized by F-SiO₂ NPs, we formed emulsions of *E. coli* culture by vortex-mixing 1 mL of the liquid culture (10⁵ cells/mL) with 6 mL of HFE-7500 containing either F-SiO₂ NPs or biocompatible EA surfactant (Raindance Technologies). The polydispersity of the drops here did not affect our measurements of cell growth. The resulting emulsions were incubated in a shaker-incubator at 37 °C and at 250 rpm. At different time points, 20 μL of the emulsions were extracted and destabilized to measure cell

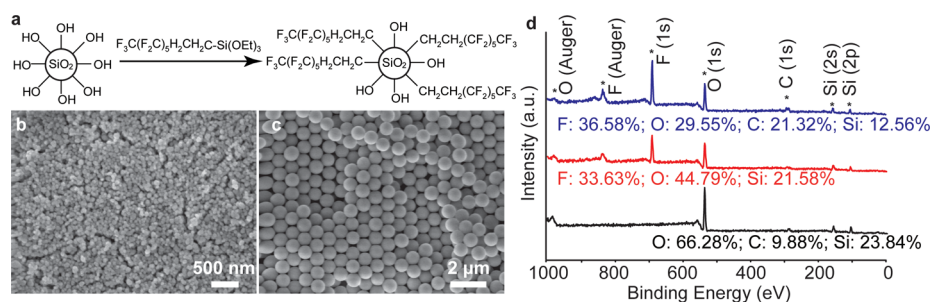


Figure 1. (a) Scheme of the fluorination process of SiO₂ NPs to form F-SiO₂ NPs. SEM images of F-SiO₂ NPs with diameters of approximately (b) 80 nm, and (c) 780 nm. (d) X-ray photoelectron spectra (XPS) of three particle samples having increasing degree of fluorination: (black curve) pristine SiO₂ before fluorination; (red curve) F-SiO₂ NPs after 60 min of fluorination where the initial 1H-1H-2H-2H perfluorooctyl triethoxysilane (FAS) concentration was at [FAS]₀ = 118.7 mM; (blue curve) F-SiO₂ NPs after 60 min of fluorination where [FAS]₀ = 502.3 mM. These three spectra correspond to samples A, B, and C, respectively, in Figure S2 (Supporting Information). Synthesis details are in Table S2 (Supporting Information).

concentrations. The emulsion was destabilized by the addition of mineral oil followed by agitation and centrifugation at low spin rate (2000–4000 rpm). The concentration of cells was measured using Thermo Scientific NanoDrop 1000 Spectrophotometer, which reports the optical density at 600 nm. The optical densities to cell concentration for *E. coli* have been calibrated by other groups.³³

2.5. Resorufin Leakage Test. Positive and negative drops were generated from flow-focusing device with serpentine channel separately. The continuous phase contained 4% (w/w) 780 nm F-SiO₂ NPs in HFE-7500. Positive drops contained 220 μM resorufin and 10 μM fluorescein in 1X PBS, and negative drops contained 1X PBS. The drops were collected separately in two Eppendorf tubes. For F-SiO₂ NPs-stabilized drops, the unadsorbed NPs in continuous phase were removed by washing with FC-40 three times before the positive and negative drops were mixed at 1:1 ratio. The presence of unadsorbed NPs was due to the fact that we used NP concentrations about 4 times higher than that needed for the complete coverage of the drops. We used an excess of particles to decrease the distance the particles must travel to reach droplet interface. EA-surfactant stabilized positive and negative drops were mixed at 1:1 ratio. The mixed drops were incubated at room temperature (293 K), and the fluorescence intensity of the droplet mixture was surveyed at different times.

2.6. Mammalian Cell Culture. MCF-7 breast carcinoma and 3T3 fibroblasts were acquired from American Tissue Culture Collection (ATCC). Cells were propagated in minimal essential medium (MEM) supplemented with 10% of fetal bovine serum (FBS for MCF7) or 10% calf bovine serum (CBS for 3T3) and passaged when cells reached ~80% confluence. For seeding on water–oil interfaces or nanoparticle-laded water–oil interfaces, the cells were detached using trypsin-EDTA for 5 min, neutralized with serum-containing medium, rinsed, and resuspended in growth medium at 25 000 cell/mL. The suspension (200 μL, 5000 cells per well) was dispensed into a well of a 96-well plate (hydrophobic polystyrene) that contained 100 μL of HFE or HFE-surfactant suspension. A two-layered system with significant curvature on the liquid–liquid interface formed spontaneously. The suspension has to be dispensed rapidly along the wall of the well as one continuous stream to avoid formation of segregated aqueous droplets. The cells were allowed to sediment onto the water–oil interface for at least 1–2 h prior to examining the cells by phase-contrast microscope (Leica) equipped with Phantom V7.3 camera (Vision Research). Experiments that used fluorescently labeled 3T3 cells were conducted similarly with one exception: the cells were incubated with 1 μg/mL solution of carboxyfluorescein succinimidyl ester (CFSE) in growth medium for 10 min, rinsed with CFSE-free medium, and allowed to recover in growth medium for 15 min prior to detachment with trypsin and seeding. The CFSE-label was stable over 3–4 days; the intensity decreased as the amount of CFSE per cell was halved at each cell division. Cells were imaged using Zeiss LSM-700 laser-scanning confocal microscope equipped with 480 nm solid-state laser, 10× or 20× objective, and the Zen software.

3. RESULTS AND DISCUSSION

3.1. Synthesis and Characterization of Amphiphilic Fluorinated Silica Nanoparticles. F-SiO₂ NPs were generated from the fluorination of presynthesized pristine SiO₂ particles with diameters ranging from 50 nm to 5 μm. The SiO₂ NPs were either synthesized using Stober method²³ or purchased and used after centrifugation. The initial size of these SiO₂ NPs determined the final size of the F-SiO₂ NPs as the fluorination process did not change the size of the particles. The SiO₂ NPs were initially hydrophilic and dispersible in the aqueous phase only. Particle surface fluorophilicity was increased by reacting the particles with 1H,1H,2H,2H-perfluorooctyltriethoxysilane (FAS) to partially derivatize the silanol groups on the surface of pristine SiO₂ NPs (Figure 1a). Details of the synthesis and fluorination are included in the Materials and Methods section. Figure 1b,c and Supporting Information show SEM images of the particles, either synthesized in-house or purchased, after the fluorination process. X-ray photoelectron spectroscopy confirmed that the particles contained fluorinated groups after the fluorination process (Figure 1d).

To identify particles that could stabilize aqueous drops in various fluorinated oils, we either varied the concentration of FAS introduced to the pristine SiO₂ NPs solution or sampled the particles at different times after the fluorination process started. We dispersed the particles in fluorinated oils and agitated the dispersion with deionized water or lysogeny broth (LB), a growth media for bacteria, to form water-in-oil emulsions. After an optimal degree of fluorination (see Table S2, Supporting Information, for details), the particles were partially wetted by both the aqueous phase and the fluororous phase. They adsorbed to the aqueous–fluororous interface and generated stable emulsions for over 24 h (Figure S2, Supporting Information). The stability of these emulsions formed by agitation was a good indicator of the stability of drops formed by microfluidic flow-focusing nozzles in subsequent experiments. Using a Wilhelmy balance (KSV NIMA, Espoo, Finland),²⁴ we measured the interfacial tension between water or LB and HFE-7500 containing various concentrations of F-SiO₂ NPs having a diameter of 52.1 ± 10 nm (from dynamic light scattering). The particles were effective in decreasing the interfacial tension between the aqueous and the fluororous phases (Figure S3, Supporting Information). The plateau in the interfacial tension values above a concentration of about 0.5% (w/w) F-SiO₂ NPs in HFE-7500 indicates that

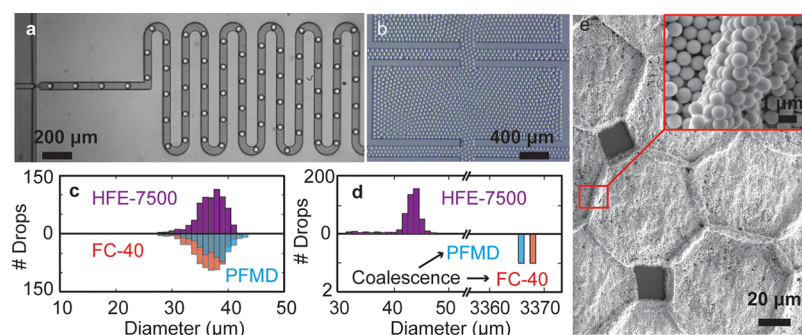


Figure 2. (a) Snapshot of drops of deionized (DI) water being generated from a flow-focusing device. The continuous phase contained 4.0% (w/w) of F-SiO₂ NPs in HFE-7500. (b) Optical image of DI water drops stabilized by F-SiO₂ NPs, being reinjected into a 55 μm tall microchannel. Histograms of drop size distribution of DI water drops before and after the continuous phase was replaced by FC-40 and perfluoromethyldecalin (PFMD), where the drops were initially stabilized by a continuous phase of (c) F-SiO₂ NPs in HFE-7500 and (d) EA-surfactant in HFE-7500. The droplet sizes were measured after incubation for 1 h and the CV increased from that when first generated at the flow-focusing nozzle. Drops stabilized by EA-surfactants coalesced into single bulk aqueous phase when resuspended in FC-40 and PFMD. (e) SEM image of nanoparticle-stabilized drops after excess particles were washed off from the continuous phase and the fluids were evaporated. The drops were about 70 μm in diameter and stabilized by 780 nm F-SiO₂ NPs; (inset) SEM image taken from the red box.

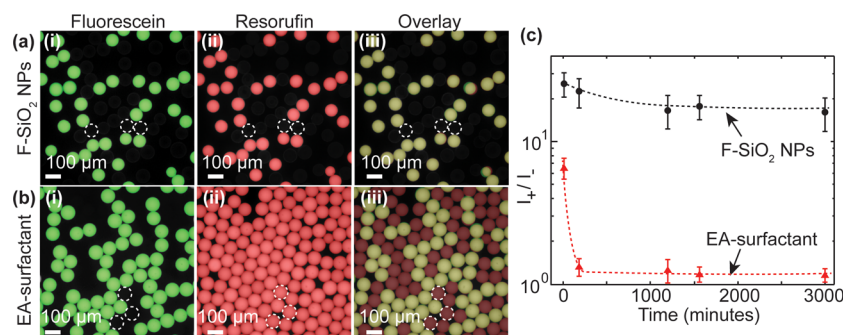


Figure 3. (a) Fluorescence images of “positive” and “negative” drops stabilized by F-SiO₂ NPs after mixing for 26 h. The emulsion contained a 1:1 mixture of “positive” drops containing fluorescein (10 μM) and resorufin (220 μM), and “negative” drops containing PBS buffer only. Fluorescein was used to tag the positive drops. Fluorescence image of (i) fluorescein, (ii) resorufin, and (iii) an overlay of fluorescein and resorufin. If there were no leakage, the fluorescein and resorufin drops should overlap in image iii and should appear yellow. Three negative drops are outlined in dashed circles. The colors were added during postprocessing of data. (b) Fluorescence images of drops stabilized by EA-surfactant after mixing for 26 h. All conditions are identical to those described for image a, except F-SiO₂ NPs are replaced by EA-surfactants. Three negative drops are outlined in dashed circles. (c) Plots of the time evolution of the ratio of resorufin fluorescence intensity of positive drops (I_+) versus that of negative drops (I_-), for drops stabilized by F-SiO₂ NPs and EA-surfactants, respectively. The mean value is calculated from 1191 F-SiO₂ NPs stabilized drops and 1064 EA-surfactant stabilized drops, respectively, and the height of the error bars represents one standard deviation from the mean. Dashed lines are fitted curves to the data.

the aqueous–fluorous interface was likely to be approaching complete coverage by nanoparticles. On the basis of the decrease in interfacial tension and an assumption that the particles at the interface were close-packed, we used an expression described by Du et al.²⁵ to estimate the desorption energy of the particles to be $\sim 10^4 k_B T$. This large value indicates that particles were likely to be irreversibly adsorbed at the interface.

3.2. Nanoparticles Are Effective Emulsifiers for Drops Generated in Microfluidic Flow-Focusing Devices. On the basis of the stability of emulsions formed by agitation (Table S2, Supporting Information), we identify particles that generated the most stable emulsions and demonstrate their compatibility with microfluidics. Similar to surfactant systems, monodisperse drops stabilized by F-SiO₂ NPs can be generated using microfluidic flow-focusing nozzles.¹⁶ Here, we focused the investigation on a single size of particles (780 nm). The use of particles of other sizes did not change our results. Particles larger than 1 μm were increasingly likely to clog the channels after prolonged operation, however. Figure 2a shows that drops

generated from a flow-focusing nozzle were monodisperse with a coefficient of variance $CV \approx 0.8\%$ (as measured at the nozzle using our imaging setup). This value is comparable with the typical value of CV for drops stabilized by surfactants. Using a single flow-focusing nozzle (nozzle dimensions: 40 × 30 μm), droplet volume was tunable from 22.4 to 127 pL by changing the flow rate (from 0.4 to 2 mL/h) of the continuous phase containing 4% (w/w) of particles in HFE-7500 (also see Figure S5, Supporting Information). We used a serpentine channel with a length of 10 to 20 cm downstream of the nozzle to ensure sufficient time for particles to adsorb to the droplet interface, such that the drops are less likely to coalesce when collected with other drops at the outlet of the channel.²⁶ These particle-stabilized drops were stable upon incubation and shaking at 100 rpm in bulk in an Eppendorf tube at 37 °C, and upon reinjection into a microchannel (Figure 2b and Figure S4, Supporting Information). They were also stable upon incubation at 95 °C for at least 20 min (Figure S6, Supporting Information). Furthermore, these drops remained intact and did not coalesce when resuspended in neat HFE-

7500, as well as perfluorinated solvents FC-40 and PFMD (Figure 2c). Such observations were consistent with the expectation that the particles were irreversibly adsorbed at the liquid–liquid interface, as the desorption energy was estimated to be $\sim 10^6 k_B T$ for particle diameter of 780 nm.^{25,27} On the other hand, the desorption energy of surfactants is typically on the order of a few $k_B T$. Drops stabilized by surfactants coalesced readily upon resuspension in perfluorinated solvents (Figure 2d). As particle-stabilized drops were stable upon resuspension in neat solvents, it was possible to wash off excess particles in the continuous phase and image the particles that were adsorbed at the aqueous–fluorous interface only. SEM images of the drops, after the aqueous and fluorous phases evaporated, show that the drops were fully covered by particles (Figure 2e, also see Figures S7 and S8, Supporting Information).

3.3. Nanoparticles Are Effective in Mitigating the Leakage of Model Dye from Drops. F-SiO₂ NPs were effective in preventing the leakage of resorufin, a model dye that is known to leak from drops stabilized by EA-surfactant.⁶ In our assay to measure leakage, two types of drops were generated. “Positive” drops contained a mixture of resorufin and fluorescein. Fluorescein is known not to leak in drops stabilized by surfactants for at least 36 h, and was thus used to tag the positive drops.^{6,28} “Negative” drops contained buffer only. By mixing the positive and negative drops, we were able to characterize the leakage of resorufin by measuring the time evolution of resorufin fluorescence intensity among positive and negative drops. Figure 3 shows that after 26 h of incubation at 20 °C, the resorufin fluorescence intensity became homogenized in drops that were stabilized by surfactants, indicating leakage of the dye. The resorufin intensity in positive drops decreased almost immediately upon mixing (Figure 3c), explaining the small ratio of resorufin fluorescence intensity of positive drops (I_+) versus that of negative drops (I_-) at the first time point at about 5 min. This ratio (I_+/I_-) decreased to a value of about 1 in less than 180 min (Figure 3c). On the contrary, the leakage of resorufin was insignificant in drops stabilized by F-SiO₂ NPs in FC-40. The value of I_+/I_- remained >15 , even after 50 h of mixing. Because nanoparticles do not form surfactant micelles, the primary role of the F-SiO₂ NPs was the elimination of such micelles, which had been reported to increase the leakage rate among aqueous droplets.⁶ We have used FC-40 instead of HFE-7500 to suspend the particles here as we observed slow leakage of resorufin when the drops were stabilized by F-SiO₂ NPs in HFE-7500, though this leakage was significantly slower than that in surfactant system (Figure S9, Supporting Information). It is known that molecules can leak from drops via multiple pathways, including the direct partitioning into the continuous phase and transport through reverse micelles.⁶ In our system, even when the NPs are close-packed on droplet surface, the presence of interstitial space between the particles could allow molecules to partition directly into the oil. Here, we suspect that resorufin might directly partition more readily into HFE-7500 (which contained an aliphatic ether group) than into FC-40 and PFMD which are completely fluorinated.⁵ We are currently testing the effectiveness of F-SiO₂ NPs in preventing the leakage of other fluorophores.

3.4. Nanoparticles Are Compatible with the Culture of *E. coli* in Drops. As a first test of biocompatibility of the nanoparticles, we compared the growth rate of *E. coli*, as measured by an increase in the optical density of cell

suspension at 600 nm (OD₆₀₀), when the cells grew (1) in contact with HFE-7500 without any surfactants or nanoparticles, (2) inside drops stabilized by the biocompatible EA-surfactant in HFE-7500, and (3) inside drops stabilized by F-SiO₂ NPs in HFE-7500. Both HFE-7500 and EA-surfactant have been shown previously to be biocompatible.^{4,29} Figure 4a

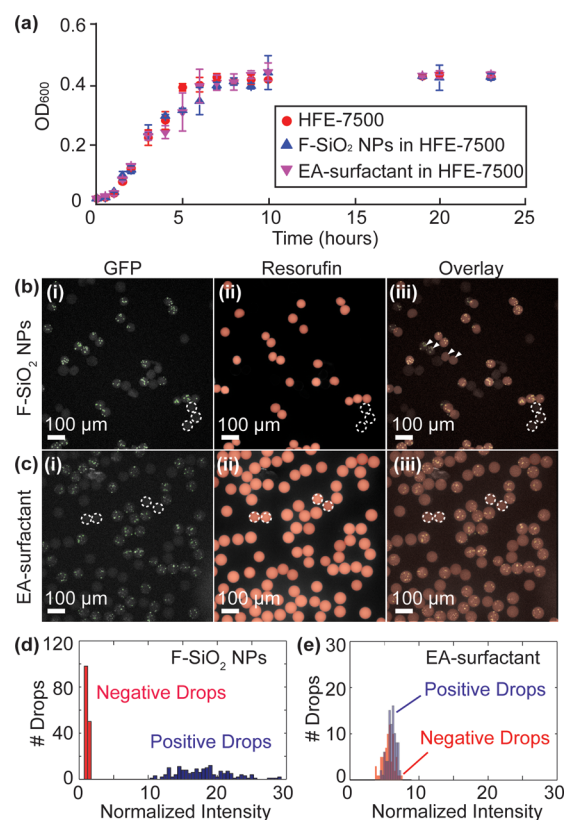


Figure 4. (a) Bacteria growth curve when the culture was suspended on top of HFE-7500, in drops stabilized by F-SiO₂ NPs in HFE-7500, and in drops stabilized by EA-surfactants in HFE-7500, respectively. The initial OD₆₀₀ value was about 0.001, and each drop contained, on average, less than one cell. The cell suspensions were incubated in a shaker-incubator at 37 °C at 250 rpm for 24 h. To measure the OD₆₀₀ from drops stabilized by F-SiO₂ NPs, we destabilized the emulsion by adding mineral oil to the emulsion followed by agitation and centrifugation to separate the aqueous phase from the fluorous phase. Drops stabilized by (b) 780 nm F-SiO₂ NPs and (c) EA-surfactants. Fluorescence images of (i) *E. coli* expressing green fluorescent protein (GFP), (ii) resorufin, and (iii) an overlay of resorufin and GFP. Positive drops containing *E. coli* expressing GFP and resazurin (60 μM) were mixed with negative drops containing buffer for 2 h. Several negative drops are outlined in dashed circles. The colors were added during postprocessing of data. The four arrows (in panel b, image iii) indicate drops that shifted in position between imaging of the resorufin and GFP. (d and e) Histograms of resorufin fluorescence intensity distribution for positive and negative drops 2 h after mixing.

shows that the growth curves of *E. coli* in all cases were indistinguishable within experimental error. This observation indicates that F-SiO₂ NPs did not affect the division of *E. coli*. In addition, Figure 4b shows that F-SiO₂ NPs did not interfere with a standard cell viability assay based on the metabolic reduction of resazurin (barely fluorescent) to resorufin (fluorescent) and that the presence of growth media (LB) and high concentrations of *E. coli* did not cause dye leakage. We

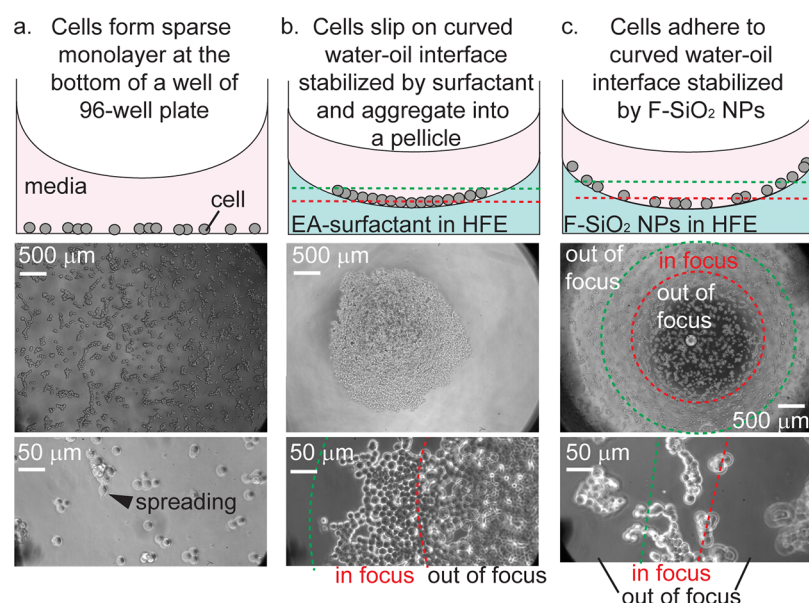


Figure 5. Adhesion or slipping of mammalian cells on curved water–oil interface. (a) Short-term adhesion of MCF-7 cells to solid surface (hydrophobic polystyrene). (b) Same number of cells plated in a well that contains curved water–oil interface. The oil consisted of EA-surfactant in HFE-7500. The cells cannot be retained on the interface, and they slip and form a curved 2D aggregate in the center of the well. (c) Same cells adhering to curved water–oil interface stabilized by F-SiO₂ NPs. The cells adhere across the entire interface and do not slip. The edge and the center of curved water–oil interface are in different focal planes. The green and red dashed lines indicated approximate borders of areas that are in focus.

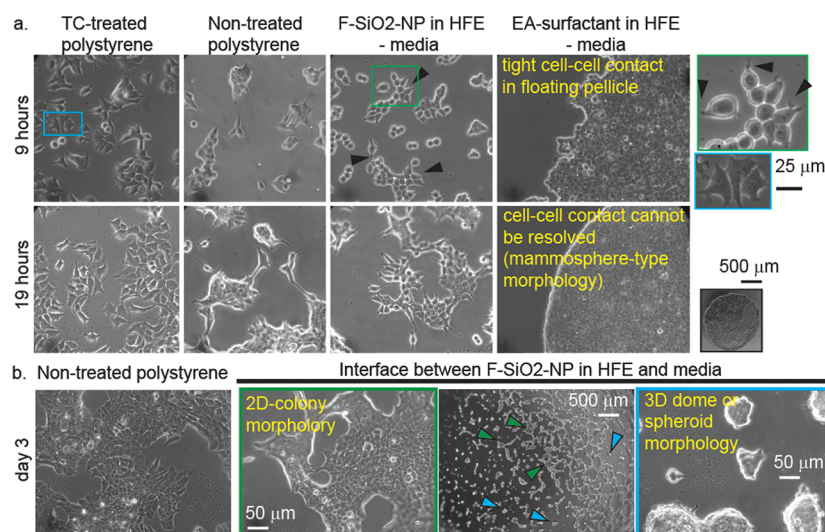


Figure 6. Short-term spreading and growth of cells on solid and liquid interfaces. (a) Dynamics of short-term spreading (19 h) of breast cancer MCF7 cells on liquid–solid and liquid–liquid interfaces in serum-containing media. On tissue-culture treated (TC) polystyrene, cells form filopodia within 3 h and spread after 5 h. Spreading is delayed on hydrophobic nontreated polystyrene; cells started to spread at 5 h and completed spreading by 19 h. Similar spreading behavior is observed on the interface of HFE-7500 stabilized by 100 nm nanoparticles. In contrast, the same liquid–liquid interface stabilized by EA-surfactant cannot support adhesion of cells; instead, cells aggregate and compact into an ellipsoid-shaped mammosphere. (b) Over the course of 3 days, MCF-7 cells fully spread and proliferate on polystyrene. Cells on nanoparticle-stabilized interface exhibit mixed morphology: they form 2D colonies composed of spread-out cells or compact 3D colonies.

used *E. coli* expressing green fluorescent protein (GFP) such that we can identify positive drops that contained *E. coli* and resazurin in LB from negative drops that contained LB only. Initially, all drops were dark because resazurin had low fluorescence levels. At time $t = 120$ min, the fluorescence intensity from positive drops stabilized by F-SiO₂ NPs increased significantly and were clearly distinguishable from the negative drops with no *E. coli* (Figure 4d). For drops stabilized by EA-surfactant, fluorescence intensity of all drops increased due to the leakage of resorufin (Figure 4e).

3.5. Nanoparticles at Liquid–Liquid Interfaces Support the Adhesion, Spreading, and Growth of Mammalian Cells. We further demonstrate that F-SiO₂ NPs were not toxic to mammalian cells and could provide a solid-like interface for the adhesion and growth of these cells. Guided by the studies with *E. coli*, we designed a toxicity assay using cells cultured in 96-well plate in the presence of 5% (v/v) HFE-7500 that contained F-SiO₂ NPs. 3T3 Fibroblasts cultured in the presence of F-SiO₂ NPs exhibited the same growth rate over 3 days as cells cultured on polystyrene without the nanoparticles

(Figure S10, Supporting Information). Neither 100 nor 780 nm nanoparticles had any effect on the rate of growth of these cells.

In addition, we observed that anchorage-dependent cells, such as fibroblasts and luminal breast carcinoma MCF-7, attached to an inclined fluorinated water–oil interface stabilized by F-SiO₂ NPs. This finding would be surprising according to previous work that showed that the interface between fluorinated oil or air and water was nonfouled by biological contaminants such as serum, blood, and biofilm-promoting bacteria cells.^{30,31} The water–oil interface is “slippery”, and such interfaces, when inclined, should not retain cells or serum proteins to which cells adhere. To investigate both adhesion and slipping, we formed a curved aqueous–fluorous interface inside individual wells in a 96-well plate by placing 100 μ L of cell suspension on top of 100 μ L of HFE-7500 containing EA-surfactant or F-SiO₂ NPs (Figure 5). The fluorous phase preferentially wets the well surface to generate a concave aqueous–fluorous interface. We have not used droplets here to facilitate imaging of cell morphology at the interface; however, we anticipate similar cell behavior on curved water–oil interfaces inside aqueous drops.

As expected, cells failed to adhere to an interface stabilized by EA-surfactant. In contrast, cells adhered to F-SiO₂ NPs-stabilized interface (Figure 5). Importantly, we observed that adherent cells spread and divided on F-SiO₂ NPs-stabilized interface (Figure 6). Cells exert contractive forces on substrates. Cell adhesion and spreading typically requires solid surfaces that can withstand contractile pulling by the cells. Fluid–fluid interfaces, including those stabilized by surfactants, cannot withstand such forces. Anchorage-dependent cells are generally not viable when suspended in a fluid.¹¹ Microscopy confirms the presence of lamellipodia and filopodia in MCF-7 cells (Figure 6b) and 3T3 fibroblasts (Figure S11, Supporting Information), suggesting that the nanoparticles must have formed stable solid-like sheets that can withstand traction forces generated by cells. These sheets were stable for multiple days as spread-out cells multiplied and created extended colonies (Figure 6 and Figure S11, Supporting Information). While it was previously suggested that water–oil interfaces stabilized by hydrophobic particles form a solid-like rigid substrate that could support the attachment of anchorage-dependent cells,¹⁵ we provide the first concrete evidence that such interfaces could, in fact, allow the adhesion, spreading, and growth of canonical anchorage-dependent fibroblasts lines. For cancer cells MCF-7, which could switch between anchorage-dependent colonies or suspended spheroids (mammospheres), nanoparticle-stabilized interface promoted the formation of adherent colonies. On the other hand, only floating-colony phenotype was observed on nanoparticle-free interfaces (Figure 6, and Figure S11, Supporting Information). Due to the low rigidity of surfactant-stabilized interfaces, the majority of previous research that combined water–oil emulsion and cell culture mandated the use of nonadherent cell lines or cells lines capable of aggregating into floating spheroid cultures.³² The rigid, solid-like interfaces described in our work can thus open up new opportunities for the culture of anchorage dependent cells.

4. CONCLUSIONS

In conclusion, we have developed a simple method for the synthesis of amphiphilic silica nanoparticles for the generation of stable aqueous droplets in a range of fluorinated oils. The particles effectively prevented the leakage of resorufin, a model

dye that was known to leak in surfactant-stabilized drops. We also showed that the particles were compatible with microfluidic flow-focusing devices. The presence of the particles did not affect the growth of *E. coli* compared with biocompatible EA-surfactant. Importantly, the particles were compatible with the growth and spreading of adherent mammalian cells, a capability not easily achievable in surfactant systems. The future evolution of droplet microfluidics hinges on the development of structurally diverse, functionalized emulsifiers for tailored applications such as interfacial reactions.³⁴ Current surfactants are limited to triblock copolymer scaffolds; such scaffolds are challenging to synthesize, purify, and characterize.³⁵ Any diversification and derivatization of these scaffolds to add any functionality to the block copolymer is not trivial. By adding NP-based emulsifiers to the repertoire of the stable emulsifiers, we open new possibilities for the design of structurally tailored emulsifiers for future applications.

■ ASSOCIATED CONTENT

Supporting Information

Detailed particle synthesis protocol and characterizations and supplementary results on leakage mitigation and biocompatibility. This material is available free of charge via the Internet at <http://pubs.acs.org>.

■ AUTHOR INFORMATION

Corresponding Author

* E-mail: sindy@stanford.edu.

Notes

The authors declare no competing financial interest.

■ ACKNOWLEDGMENTS

We acknowledge funding from the Stanford Nano Shared Facilities Bio/Medical Mini Seed Grant and the Stanford Woods Institute for the Environment. S.T. acknowledges additional support from 3M Untenured Faculty Award. R.D. acknowledges the Canadian Foundation for Innovation for infrastructure support and NSERC Discovery Grant. E.L. acknowledges the Alberta Innovates Health Solutions (AIHS) Summer Fellowship and the Lloyd and Margaret Cooley Memorial Studentship in Analytical Chemistry.

■ REFERENCES

- (1) Kiss, M. M.; Ortoleva-Donnelly, L.; Beer, N. R.; Warner, J.; Bailey, C. G.; Colston, B. W.; Rothberg, J. M.; Link, D. R.; Leamon, J. H. High-Throughput Quantitative Polymerase Chain Reaction in Picoliter Droplets. *Anal. Chem.* **2008**, *80*, 8975–8981.
- (2) Agresti, J. J.; Antipov, E.; Abate, A. R.; Ahn, K.; Rowat, A. C.; Baret, J.-C.; Marquez, M.; Klivanov, A. M.; Griffiths, A. D.; Weitz, D. A. Ultrahigh-Throughput Screening in Drop-based Microfluidics for Directed Evolution. *Proc. Natl. Acad. Sci. U.S.A.* **2010**, *107*, 4004–4009.
- (3) Boedicker, J. Q.; Li, L.; Kline, T. R.; Ismagilov, R. F. Detecting Bacteria and Determining Their Susceptibility to Antibiotics by Stochastic Confinement in Nanoliter Droplets Using Plug-based Microfluidics. *Lab Chip* **2008**, *8*, 1265–1272.
- (4) Holtze, C.; Rowat, A. C.; Agresti, J. J.; Hutchison, J. B.; Angile, F. E.; Schmitz, C. H. J.; Koster, S.; Duan, H.; Humphry, K. J.; Scanga, R. A.; Johnson, J. S.; Pisignano, D.; Weitz, D. A. Biocompatible Surfactants for Water-in-Fluorocarbon Emulsions. *Lab Chip* **2008**, *8*, 1632–1639.
- (5) Mazutis, L.; Baret, J.-C.; Treacy, P.; Skhiri, Y.; Araghi, A. F.; Ryckelynck, M.; Taly, V.; Griffiths, A. D. Multi-Step Microfluidic

Droplet Processing: Kinetic Analysis of an in Vitro Translated Enzyme. *Lab Chip* **2009**, *9*, 2902–2908.

(6) Skhiri, Y.; Gruner, P.; Semin, B.; Brosseau, Q.; Pekin, D.; Mazutis, L.; Goust, V.; Kleinschmidt, F.; El Harrak, A.; Hutchison, J. B.; Mayot, E.; Bartolo, J.-F.; Griffiths, A. D.; Taly, V.; Baret, J.-C. Dynamics of Molecular Transport by Surfactants in Emulsions. *Soft Matter* **2012**, *8*, 10618–10627.

(7) Woronoff, G.; El Harrak, A.; Mayot, E.; Schicke, O.; Miller, O. J.; Soumillion, P.; Griffiths, A. D.; Ryckelynck, M. New Generation of Amino Coumarin Methyl Sulfonate-Based Fluorogenic Substrates for Amidase Assays in Droplet-based Microfluidic Applications. *Anal. Chem.* **2011**, *83*, 2852–2857.

(8) Chen, Y.; Gani, A. W.; Tang, S. K. Y. Characterization of Sensitivity and Specificity in Leaky Droplet-based Assays. *Lab Chip* **2012**, *12*, 5093–5103.

(9) Sandoz, P. A.; Chung, A. J.; Weaver, W. M.; Di Carlo, D. Sugar Additives Improve Signal Fidelity for Implementing Two-Phase Resorufin-based Enzyme Immunoassays. *Langmuir* **2014**, *30*, 6637–6643.

(10) Rosenfeld, L.; Lin, T.; Derda, R.; Tang, S. K. Y. Review and Analysis of Performance Metrics of Droplet Microfluidics Systems. *Microfluid. Nanofluid.* **2014**, *16*, 921–939.

(11) Discher, D. E.; Janmey, P.; Wang, Y. L. Tissue Cells Feel and Respond to the Stiffness of Their Substrate. *Science* **2005**, *310*, 1139–1143.

(12) Du, G.-S.; Pan, J.-Z.; Zhao, S.-P.; Zhu, Y.; den Toonder, J. M. J.; Fang, Q. Cell-based Drug Combination Screening with a Microfluidic Droplet Array System. *Anal. Chem.* **2013**, *85*, 6740–7.

(13) Lee, Y. Y.; Narayanan, K.; Gao, S. J.; Ying, J. Y. Elucidating Drug Resistance Properties in Scarce Cancer Stem Cells using Droplet Microarray. *Nano Today* **2012**, *7*, 29–34.

(14) Platzman, I.; Janiesch, J.-W.; Spatz, J. P. Synthesis of Nanostructured and Biofunctionalized Water-in-Oil Droplets as Tools for Homing T Cells. *J. Am. Chem. Soc.* **2013**, *135*, 3339–3342.

(15) Dinsmore, A. D.; Hsu, M. F.; Nikolaidis, M. G.; Marquez, M.; Bausch, A. R.; Weitz, D. A. Colloidosomes: Selectively Permeable Capsules Composed of Colloidal Particles. *Science* **2002**, *298*, 1006–1009.

(16) Anna, S. L.; Bontoux, N.; Stone, H. A. Formation of Dispersions using “Flow Focusing” in Microchannels. *Appl. Phys. Lett.* **2003**, *82*, 364–366.

(17) Pickering, S. U. CXCVI.—Emulsions. *J. Chem. Soc., Trans.* **1907**, *91*, 2001–2021.

(18) Subramaniam, A. B.; Abkarian, M.; Stone, H. A. Controlled Assembly of Jammed Colloidal Shells on Fluid Droplets. *Nat. Mater.* **2005**, *4*, 553–556.

(19) Crossley, S.; Faria, J.; Shen, M.; Resasco, D. E. Solid Nanoparticles that Catalyze Biofuel Upgrade Reactions at the Water/Oil Interface. *Science* **2010**, *327*, 68–72.

(20) Pustovit, V. N.; Shahbazyan, T. V. Fluorescence Quenching Near Small Metal Nanoparticles. *J. Chem. Phys.* **2012**, *136*, 204701.

(21) Wang, H.; Fang, J.; Cheng, T.; Ding, J.; Qu, L.; Dai, L.; Wang, X.; Lin, T. One-Step Coating of Fluoro-Containing Silica Nanoparticles for Universal Generation of Surface Superhydrophobicity. *Chem. Commun.* **2008**, *0*, 877–879.

(22) Yildirim, A.; Budunoglu, H.; Daglar, B.; Deniz, H.; Bayindir, M. One-Pot Preparation of Fluorinated Mesoporous Silica Nanoparticles for Liquid Marble Formation and Superhydrophobic Surfaces. *ACS Appl. Mater. Interfaces* **2011**, *3*, 1804–1808.

(23) Stöber, W.; Fink, A.; Bohn, E. Controlled Growth of Monodisperse Silica Spheres in the Micron Size Range. *J. Colloid Interface Sci.* **1968**, *26*, 62–69.

(24) Butt, H.-J.; Graf, K.; Kappl, M. Contact Angle Phenomena and Wetting. In *Physics and Chemistry of Interfaces*; Wiley-VCH Verlag GmbH & Co. KGaA: Weinheim, 2004; pp 118–144.

(25) Du, K.; Glogowski, E.; Emrick, T.; Russell, T. P.; Dinsmore, A. D. Adsorption Energy of Nano- and Microparticles at Liquid–Liquid Interfaces. *Langmuir* **2010**, *26*, 12518–12522.

(26) Kotula, A. P.; Anna, S. L. Probing Timescales for Colloidal Particle Adsorption using Slug Bubbles in Rectangular Microchannels. *Soft Matter* **2012**, *8*, 10759–10772.

(27) Pieranski, P. Two-Dimensional Interfacial Colloidal Crystals. *Phys. Rev. Lett.* **1980**, *45*, 569–572.

(28) Tjhung, K. F.; Burnham, S.; Anany, H.; Griffiths, M. W.; Derda, R. Rapid Enumeration of Phage in Monodisperse Emulsions. *Anal. Chem.* **2014**, *86*, 5642–5648.

(29) Clausell-Tormos, J.; Lieber, D.; Baret, J. C.; El-Harrak, A.; Miller, O. J.; Frenz, L.; Blouwolf, J.; Humphry, K. J.; Koster, S.; Duan, H.; Holtze, C.; Weitz, D. A.; Griffiths, A. D.; Merten, C. A. Droplet-based Microfluidic Platforms for the Encapsulation and Screening of Mammalian Cells and Multicellular Organisms. *Chem. Biol.* **2008**, *15*, 427–437.

(30) Wong, T. S.; Kang, S. H.; Tang, S. K. Y.; Smythe, E. J.; Hatton, B. D.; Grinthal, A.; Aizenberg, J. Bioinspired Self-Repairing Slippery Surfaces with Pressure-Stable Omniphobicity. *Nature* **2011**, *477*, 443–447.

(31) Epstein, A. K.; Wong, T.-S.; Belisle, R. A.; Boggs, E. M.; Aizenberg, J. Liquid-Infused Structured Surfaces with Exceptional Anti-Biofouling Performance. *Proc. Natl. Acad. Sci. U.S.A.* **2012**, *109*, 13182–13187.

(32) Chan, H. F.; Zhang, Y.; Ho, Y.-P.; Chiu, Y.-L.; Jung, Y.; Leong, K. W. Rapid Formation of Multicellular Spheroids in Double-Emulsion Droplets with Controllable Microenvironment. *Sci. Rep.* **2013**, *3*, 3462.

(33) Sezonov, G.; Joseleau-Petit, D.; D’Ari, R. *Escherichia coli* Physiology in Luria–Bertani Broth. *J. Bacteriol.* **2007**, *189*, 8746–8749.

(34) Theberge, A. B.; Courtois, F.; Schaerli, Y.; Fischlechner, M.; Abell, C.; Hollfelder, F.; Huck, W. T. S. Microdroplets in Microfluidics: An Evolving Platform for Discoveries in Chemistry and Biology. *Angew. Chem., Int. Ed.* **2010**, *49*, 5846–5868.

(35) Matochko, W. L.; Ng, S.; Jafari, M. R.; Romaniuk, J.; Tang, S. K. Y.; Derda, R. Uniform Amplification of Phage Display Libraries in Monodisperse Emulsions. *Methods* **2012**, *58*, 18–27.